Design and Analysis of a MEMS-Based Electrothermal Microgripper

Marija Cauchi, Pierluigi Mollicone, Ivan Grech, Bertram Mallia, Nicholas Sammut

Department of Mechanical Engineering, and Department of Metallurgy & Materials Engineering, Faculty of Engineering, University of Malta, Malta

Department of Microelectronics and Nanoelectronics, Faculty of Information & Communication Technology, University of Malta, Malta

Email: **mcauc03@um.edu.mt**

Web: **www.um.edu.mt**

Summary

Microelectromechanical systems (MEMS) have established themselves in various science and engineering domains. MEMS-based microgrippers provide several advantages in terms of compact size and low cost, and they play vital roles in microassembly and micromanipulation fields within both micromanufacturing and biological sectors. Microactuators based on different actuation principles have been devised to drive MEMS microgrippers.

This paper presents a finite element model of a MEMS-based electrothermally actuated microgripper performed using CoventorWare®. The microgripper design follows standard micromachining processes that make use of reactive ion etching where polysilicon acts as the main structural material while a chromium and gold layer is deposited on the structure for thermal actuation. The simulations are used to assess the performance of the microgripper and to optimise its operating parameters.

Keywords

microelectromechanical systems, microgripper, electrothermal actuation, finite element model

Introduction

Microelectromechanical systems (MEMS) are microscopic devices that consist of a microelectronic part and a miniaturised mechanical part embedded on the same semiconductor package using microfabrication techniques. The compact size and low cost of MEMS have given them key applications in various science and engineering domains [1]. Microgrippers are typical MEMS devices and are widely used in microassembly and micromanipulation fields. They serve to handle and manipulate micro-objects, such as micromechanical parts and biological cells, without causing damage [2, 3].

An essential component of all active MEMS is a microactuator that ensures the necessary motions to make the device operational. Different actuation methods include shape-memory alloys, electrostatic, electrothermal, piezoelectric, pneumatic, and electromagnetic approaches. Electrothermal actuators have several advantages in that they can generate a relatively large output force and displacements with a small applied voltage. Their operational principle relies on thermal expansion due to resistive heating [4].

This paper presents the design of a MEMS-based electrothermal microgripper whose analytical and numerical models are developed to study its behaviour and its principle of operation. The fabrication process implemented within the numerical model is described together with the finite element analysis performed with CoventorWare®. Different microgripper designs are explored with emphasis on optimal design and performance key factors including temperature and maximum deflection.

Microgripper Design

Structure of the Microgripper

The microgripper presented in this paper is based on the well-established 'hot and cold arm' actuator design. The 'hot and cold arm' actuator is composed of two parallel arms of different widths that are joined at their free ends to form a U-shape electrical loop [5]. Two 'hot and cold arm' actuators are then placed anti-symmetrically next to each other to form the microgripper (Fig. 1).

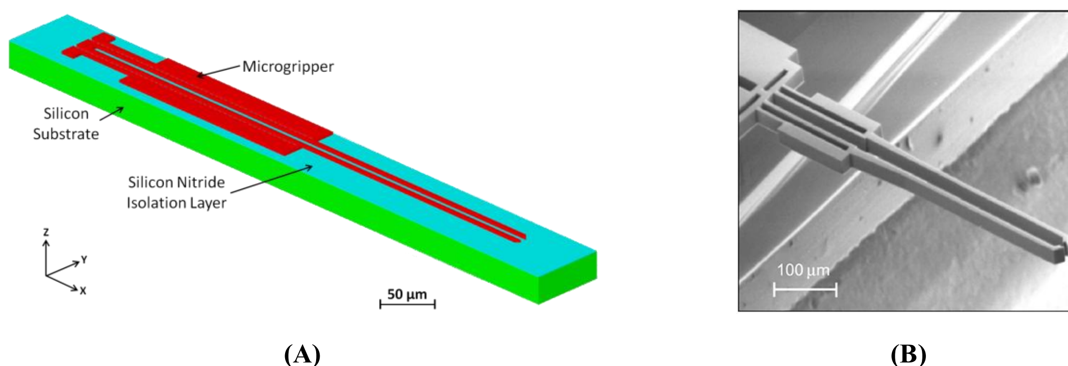

(A) **(B)**

Figure 1: MEMS-based electrothermal microgripper. (A) An oblique view of the 3D 'hot and cold arm' microgripper in CoventorWare®. The heights of the silicon substrate and the silicon nitride layer are 20 µm and 0.6 µm respectively. The height of the air gap between the suspended polysilicon microgripper and the silicon nitride layer is 2 µm. (B) A scanning electron micrograph of a fabricated overhanging microgripper [6].

The microgripper design (Fig. 2) consists of the following key elements [5]:

1. **Anchor Pads**: Their function is to anchor the microgripper to the substrate. They also serve as junctions where the driving voltage is applied.
2. **Hot and Cold Arms**: These are the main components of the microgripper. The narrower arm experiences greater heating and expansion than the wider arm, resulting in lateral bending of the actuator tip.
3. **Flexure**: This connects the anchor pad to the cold arm, and aids the flexibility in the direction of motion. Together with the hot arm, the flexure has to be designed in such a way that its cross-sectional area is as minimum as possible considering the capability of the fabrication process.

4. **Gripping Arms**: These two flexible arms are driven by the 'hot and cold arm' electrothermal microactuators to open and close as necessary.

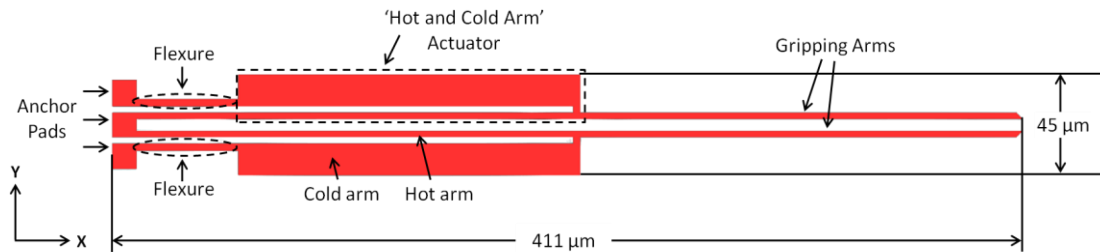

Figure 2: Top view of the microgripper design with markings of the key elements. The initial separation distance of the two gripper arms is 5 µm in this design.

Principal of Operation

Thermal expansion of the hot and cold arms is achieved through resistive heating of the suspended polysilicon structure. A thin metal layer attached selectively on top of the polysilicon beam serves to decrease the resistance. This leads to an increase in the current density which results in more heating and thus greater expansion. Under an electric current load, the narrow arm heats and expands more than the wide arm, thereby bending the structure. The actuator movement is influenced by the temperature difference between the narrower (and hotter) arm segment and the wider (and colder) arm segment. Increasing this temperature difference improves the efficiency of the actuator.

Since the actuator beam length is much longer than its width or height, a one-dimensional (1-D) analysis is deemed sufficient to model the longitudinal heat flow along the polysilicon beam [7]. Fig. 3 illustrates a 1-D differential element with height h, width w and thickness dx showing the heat generation due to the applied potential, the conduction heat loss to the adjacent connected elements, and the conduction heat loss through the air gap and into the substrate.

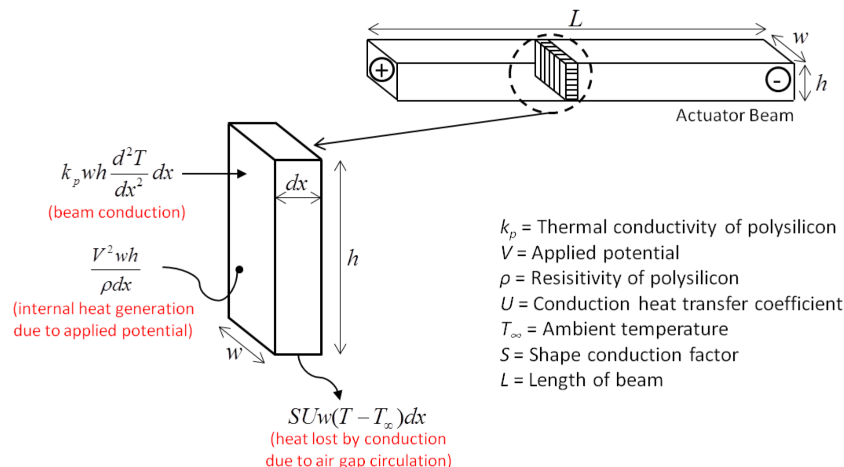

Figure 3: 1-D differential element for thermal analysis of the polysilicon beam. The internal heat generation is dissipated by means of conduction through the polysilicon beam, and through the air gap to the substrate.

Due to the very small gap between the substrate and the polysilicon beam (t_v = 2 µm), conduction from the beam's bottom surface through the air to the substrate dominates, and heat transfer by free convection and radiation can be reasonably ignored [5, 8]. Moreover, conduction from the sides of the beam through the surrounding air to the substrate is not negligible and must be accounted for by the shape conduction factor S [7].

Assuming purely conductive heat transfer from the surface of the thermal actuator to the air, and approximating the heat transfer coefficient U as a constant (~15000 W/m^{2}K for air and an air gap of 2 µm), the maximum change in temperature of the hot arm, ΔT_{max}, can be approximated by Eq. (1) [8]:

$$\Delta T_{\max} = \frac{V^2}{SUwRL} \quad \text{... Eq. (1)}$$

where V is the voltage across the hot arm, R is the resistance of the hot arm, w and L are the width and length of the hot arm respectively, and S is the shape conduction factor given by Eq. (2) [5, 7]:

$$S = \frac{h}{w}\left(\frac{2t_v}{h} + 1\right) + 1 \quad \text{... Eq. (2)}$$

The expansion of the hot arm causes the cold arm and flexure components to also expand slightly, thus reducing the net expansion difference between the hot arm and the cold arm/flexure components. The net temperature difference, ΔT_{net}, is defined as the temperature difference which would cause the same net expansion if applied to the hot arm alone and is given by Eq. (3) [8]:

$$\Delta T_{net} = \frac{1}{L_1}\left[\int_0^{L_1} T_{hot}dx - \int_0^{L_2} T_{cold}dx - \int_0^{L_3} T_{flex}dx\right] \quad \text{... Eq. (3)}$$

where L_1, L_2 and L_3 are the lengths, and T_{hot}, T_{cold} and T_{flex} are the average temperatures, of the hot arm, cold arm, and flexure components respectively.

Assuming that the hot arm and flexure components have the same cross-sectional area A and the same moment of inertia I, the elastic deflection at the tip of the actuator, δy, is given by Eq. (4) [8]:

$$\partial y = \frac{1}{2}\cdot\left[\frac{(a^4 - a^2 + 2a)Ar\alpha\Delta T_{net}L^2}{5a^4I + a^4r^2A - 2a^3I + 5aI + r^2aA + I + a^5I - 2a^2I}\right] \quad \text{... Eq. (4)}$$

where a is the ratio of the flexure length to the hot arm length, r is the centre spacing between the hot arm and the flexure, L is the length of the hot arm, and α is the coefficient of thermal expansion.

Fabrication Process

The fabrication process implemented within the microgripper model is the PolyMUMPs process. This is a 3-layer polysilicon surface micromachining process in which the layers are deposited using low pressure chemical vapour deposition (Fig. 4). Polysilicon acts as the main structural material, deposited oxide is used as the sacrificial layer while a metal layer is deposited on top of the structure for thermal actuation. The silicon nitride layer serves as electrical isolation between the polysilicon and the substrate.

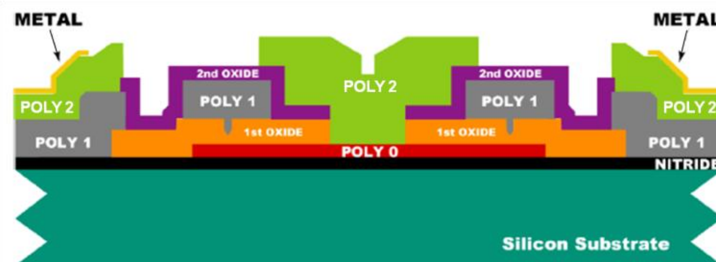

Figure 4: Schematic cross-sectional view of all layers of the PolyMUMPs process (not-to-scale). The thickness of the Poly1, Poly2 and Metal Layers are 2 µm, 1.5 µm and 0.5 µm respectively [9].

The polysilicon layers are patterned by lithography which includes the coating of the wafers with photoresist, exposure of the photoresist with the appropriate mask, and development of the exposed photoresist to create the desired etch mask. Subsequent pattern transfer into the underlying layer is achieved through reactive ion etching. The oxide layers are removed at the end of the process by immersing the chips in a hydrofluoric solution to free the mechanical polysilicon layers.

Finite Element Analysis

A numerical model that considers and solves for the combined electrical, thermal, and mechanical behaviour of the designed microgripper has been developed. The model can be divided into two sections: electrothermal analysis and thermomechanical analysis. The solver uses the material properties specified in the model's database to compute the electro-thermo-mechanical solution.

The electrothermal analysis consists of converting the potential distribution values calculated by the solver to data points that reflect the Joule heating effects resulting from the current. The solver determines the temperature distribution and applies the computed temperature values along the actuator beams. The thermomechanical analysis then uses the increase in beam temperatures to compute the thermal strain and employs the method of virtual work to predict deflection.

A preliminary assessment of the microgripper performance under an applied potential is done by evaluating the maximum temperature reached within the polysilicon hot arm. The applied thermal boundary conditions include the temperature boundary conditions and the conduction heat transfer coefficient applied on the bottom and side surfaces of the hot arm (Fig. 5A). Numerical results of the maximum temperature reached on the hot arm are found to closely agree with analytical results calculated using Eq. (1), with the difference in values being less than 5% (Fig. 5B).

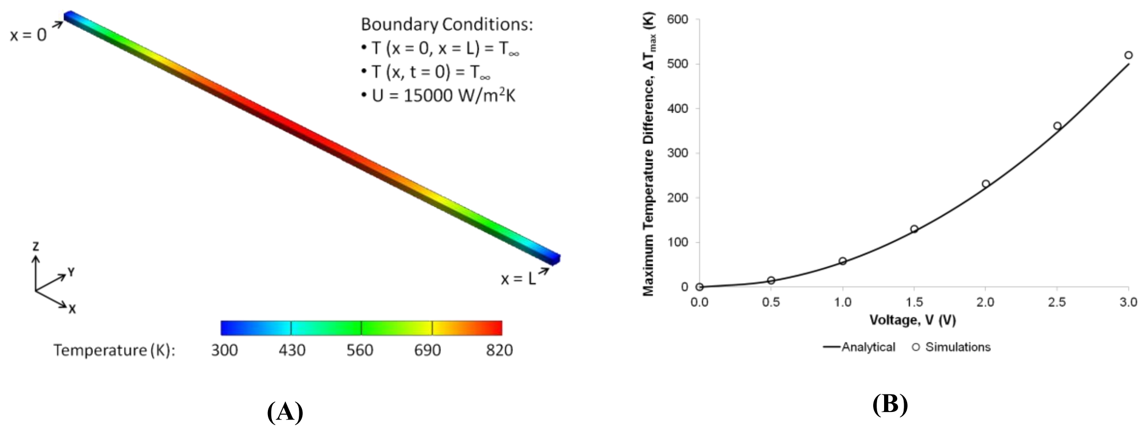

(A) **(B)**

Figure 5: Simulated steady-state temperature profile under an applied potential of 3V across the polysilicon (Poly1) hot arm. (A) Temperature plot at 3V. (B) Analytical and numerical results for maximum temperature on the hot arm as a function of applied potential.

Fig. 6 shows the temperature profile along the hot arm, cold arm and flexure components of the polysilicon actuator where the average temperature of each arm can be obtained from the area under the respective arm curve. From the areas under the curve in Fig. 6B and using Eq. (3), ΔT_{net} was found to be equal to $0.37\Delta T_{max}$. This is in agreement with literature where it is stated that ΔT_{net} is typically 1/2 to 1/3 of ΔT_{max} [8].

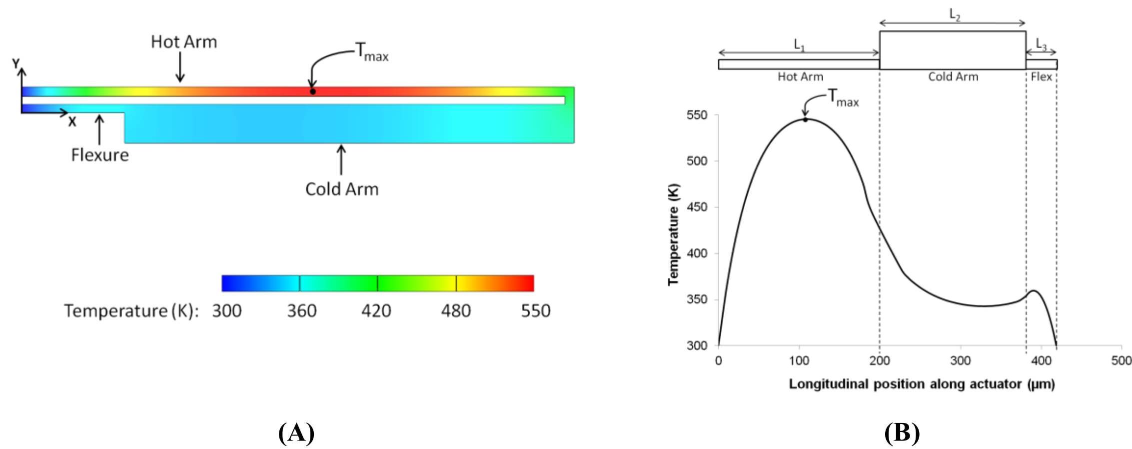

(A) **(B)**

Figure 6: Simulated steady-state temperature profile of the polysilicon (Poly1) thermal actuator subjected to an applied potential of 3V. (A) Temperature plot at 3V. The maximum temperature is 546°C and is located near the middle of the hot arm. (B) Temperature profile along the hot arm, cold arm and flexure components at 3V. For illustration purposes, the diagram above the graph shows the actuator as if it were unfolded.

The different thermal expansions of the hot and cold arms upon applying a potential across the actuator cause the tip of the actuator to move laterally in an arching motion towards the 'cold' arm side (Fig. 7A). Numerical results of the lateral (y-direction) displacement of one polysilicon 'hot and cold arm' actuator are found to closely agree with analytical results determined using Eq. (4), with a difference in values of less than 10% (Fig. 7B).

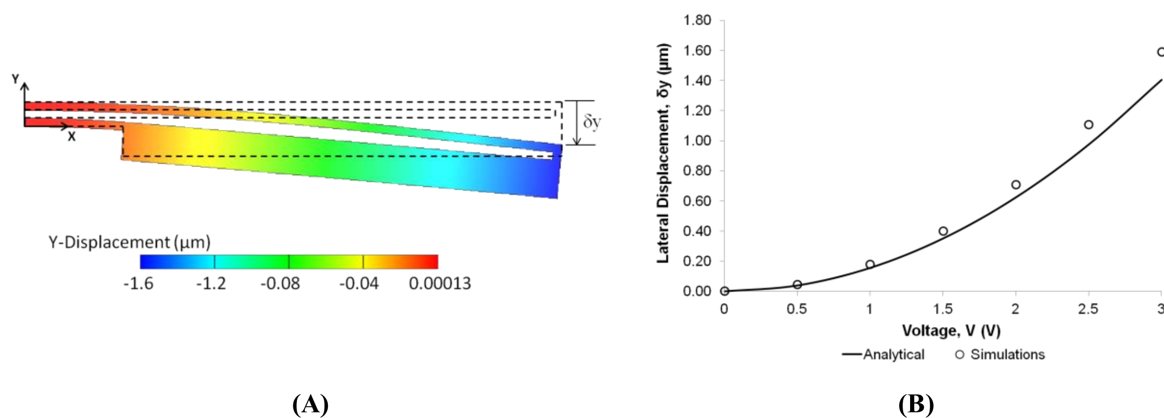

(A) **(B)**

Figure 7: Simulated steady-state lateral displacement profile of the polysilicon (Poly1) thermal actuator subjected to an applied potential of 3V. (A) Lateral displacement plot at 3V. The dotted line indicates the original actuator position at no applied potential. (B) Analytical and numerical results for lateral displacement as a function of voltage.

Eq. (4) depicts that one of the design parameters that influences the maximum deflection of the actuator is the ratio of the flexure length to the hot arm length, a. Fig. 8A shows the variation of δy with a for ΔT_{max} = 100K and L_1 = 200 µm. A maximum temperature difference of 100K is chosen as this is the maximum allowed operating temperature of the microgripper for the manipulation of living cells and tissues. A full microgripper with two 'hot and cold arm' actuators was then modelled in CoventorWare® using an optimised a value of 0.23. An optimised a parameter ascertains that the flexure is designed long enough to ensure proper elastic deflection of the actuator. The full microgripper design is composed of two layers of polysilicon with a metal layer deposited on top (Fig. 8B). The metal layer consists of a thin adhesion layer of chromium (Cr) and 0.5 µm of gold (Au).

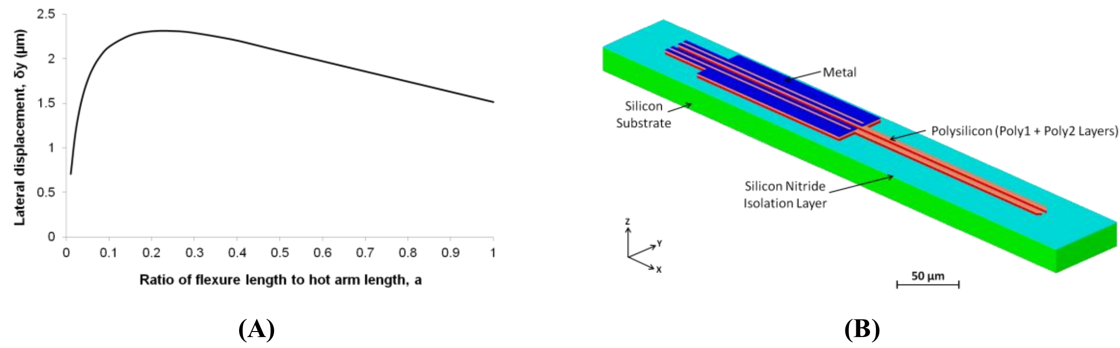

Figure 8: Microgripper design with optimised physical geometry. (A) Variation of lateral displacement with a for the 'hot and cold arm' actuator with Poly1, Poly2 and Metal for ΔT_{max} = 100K and L_1 = 200 µm. (B) An oblique view of the 3D microgripper with two layers of polysilicon with a metal layer deposited on top.

An applied voltage of 0.22V is required to obtain a ΔT_{max} of 100K for the microgripper with 2 layers of polysilicon and a metal layer on top. The performance of the microgripper with Poly1 only is compared with that of the microgripper with Poly1, Poly2 and Metal (Fig. 9). Much larger displacements are achieved for the same applied voltage in the latter case since the thin metal (Cr/Au) layer results in better thermal actuation. Moreover, by optimising the metal deposition and depositing the metal layer on top of the hot arm only, the temperature difference between the hot and cold arms is increased as the cold arm is not subject to any heating (Fig. 9). In such a design with optimised metal deposition, the maximum stresses are developed within the metal layer. A maximum Von Mises stress value of 133 MPa is developed at the same location where the maximum temperature is reached on the hot arm.

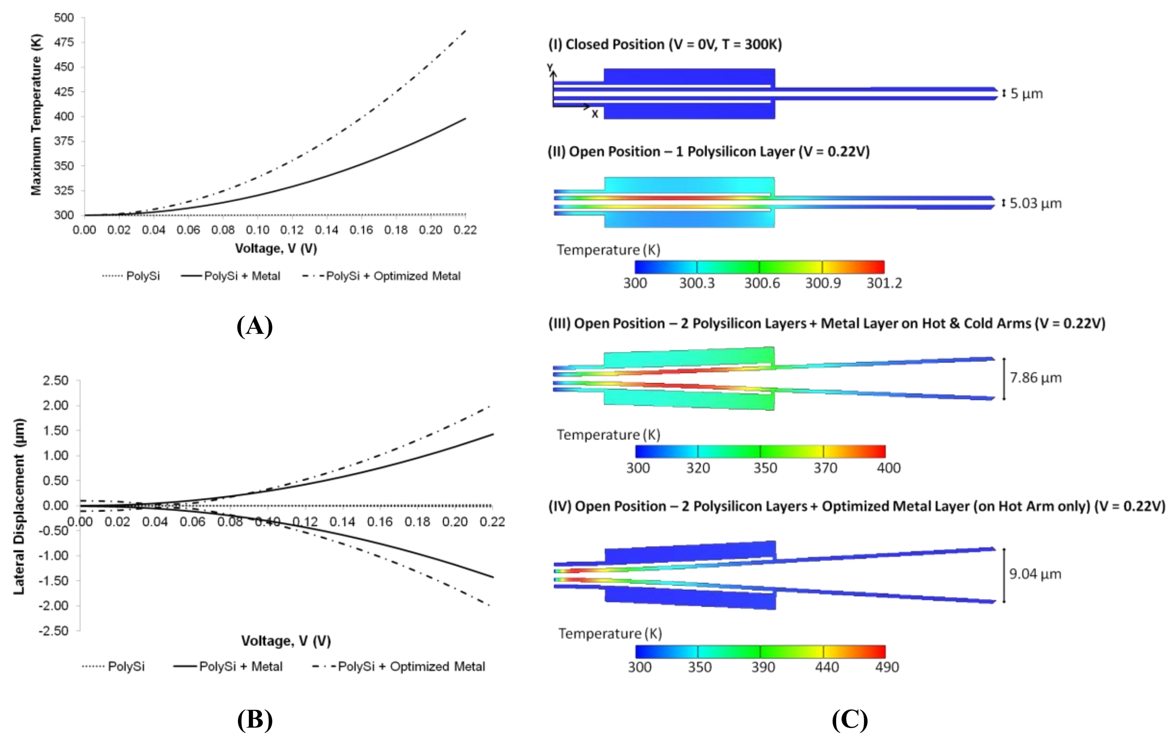

Figure 9: Comparison of the performance of the microgripper with polysilicon only, polysilicon and metal, and polysilicon and optimised metal (deposited on hot arm only) at an applied potential of 0.22V. The gap opening in the closed position is 5 µm. (A) Variation of maximum temperature with voltage. (B) Variation of lateral displacement with voltage. (C) Closed and open microgripper positions for the different scenarios (not-to-scale).

Conclusions

This paper has presented a finite element model of an electrothermal microgripper developed with CoventorWare®. With relatively low voltage requirements and high force output, electrothermal actuation has several advantages over other actuation mechanisms. The operating principle of an electrothermal microgripper with lateral motion (parallel to the substrate) is the asymmetrical thermal expansion of a microstructure with variable cross-sections. This differential thermal expansion causes the actuator to move laterally, with the flexure part aiding the flexibility in the direction of motion.

The fabrication process implemented within the model was the PolyMUMPs process that uses different polysilicon layers with a metal layer deposited on top for optimised thermal actuation. Finite element analysis was applied to simulate and evaluate the performance of the designed microgripper. Numerical results for maximum temperature and elastic lateral deflection were found to closely agree with analytical values. The electrothermal principle relates the deflection of the actuator to various process parameters, the physical geometry of the actuator as well as the driving current. Optimal geometrical dimensions and different metal depositions were implemented to optimise the actuator structure and its operating parameters. The temperature distribution and the deflection of the microgripper were the key factors compared in the range of microactuator functionality.

Acknowledgements

The research work disclosed in this publication is funded by the REACH HIGH Scholars Programme – Post-Doctoral Grants. The grant is part-financed by the European Union, Operational Programme II – Cohesion Policy 2014-2020 Investing in human capital to create more opportunities and promote the wellbeing of society – European Social Fund.

References

[1] S. Senturia, *Microsystem Design*, Springer US, Chapter: Introduction, pp. 3-14, 2001.

[2] R. Zhang et al., "A Multipurpose Electrothermal Microgripper for Biological Micro-Manipulation", *Microsyst. Tech.*, vol. 19, no. 1, pp. 89-97, 2013.

[3] K. Ivanova et al., "Thermally Driven Microgripper as a Tool for Micro Assembly", *Microelectronic Engineering*, vol. 83, no. 4-9, pp. 1393-1395, 2006.

[4] Y. Jia and Q. Xu, "MEMS Microgripper Actuators and Sensors: The State-of-the-Art Survey", *Recent Patents on Mechanical Engineering*, vol. 6, no. 2, pp. 132-142, 2013.

[5] Q. A. Huang and N. K. S. Lee, "Analysis and Design of Polysilicon Thermal Flexure Actuator", *J. Micromech. Microeng.*, vol. 9, pp. 64-70, 1999.

[6] N. Chronis and L.P. Lee, "Electrothermally Activated SU-8 Microgripper for Single Cell Manipulation in Solution", *J. Microelectromech. Syst.*, vol. 14, no. 4, pp. 857-863, 2005.

[7] L. Lin and M. Chiao, "Electrothermal Responses of Lineshape Microstructures", *Sens. Actuators A,* vol. 55, no. 1, pp. 35-41, 1996.

[8] R. Hickey, M. Kujath, and T. Hubbard, "Heat Transfer Analysis and Optimization of Two-Beam Microelectromechanical Thermal Actuators", *J. Vac. Sci. Technol. A*, vol.20, no.3, pp. 971-974, 2002.

[9] A. Cowen et al., "PolyMUMPs Design Handbook", MEMSCAP Inc., Revision 13.0.

View publication stats